

PROVABLE MAXIMUM ENTROPY MANIFOLD EXPLORATION VIA DIFFUSION MODELS

Riccardo De Santi^{1,2,†}, Marin Vlastelica^{1,2,†}, Ya-Ping Hsieh¹, Zebang Shen¹, Niao He^{1,2}, Andreas Krause^{1,2 *}

¹ ETH Zurich, ² ETH AI Center

{rdesanti, niaohe, krausea}@ethz.ch

{marin.vlastelica, yaping.hsieh, zebang.shen}@inf.ethz.ch

ABSTRACT

Exploration is critical for solving real-world decision-making problems such as scientific discovery, where the objective is to generate truly novel designs rather than mimic existing data distributions. In this work, we address the challenge of leveraging the representational power of generative models for exploration without relying on explicit uncertainty quantification. We introduce a novel framework that casts exploration as entropy maximization over the approximate data manifold implicitly defined by a pre-trained diffusion model. Then, we present a novel principle for exploration based on density estimation, a problem well-known to be challenging in practice. To overcome this issue and render this method truly scalable, we leverage a fundamental connection between the entropy of the density induced by a diffusion model and its score function. Building on this, we develop an algorithm based on mirror descent that solves the exploration problem as sequential fine-tuning of a pre-trained diffusion model. We prove its convergence to the optimal exploratory diffusion model under realistic assumptions by leveraging recent understanding of mirror flows. Finally, we empirically evaluate our approach on both synthetic and high-dimensional text-to-image diffusion, demonstrating promising results.

1 INTRODUCTION

Recent progress in generative modeling, particularly the emergence of diffusion models (Sohl-Dickstein et al., 2015; Song & Ermon, 2019; Ho et al., 2020), has achieved unprecedented success in generating high-quality samples across diverse domains, including chemistry (Hoogeboom et al., 2022), biology (Corso et al., 2022), and robotics (Chi et al., 2023). Traditionally, generative models have been employed to capture the underlying data distribution in high-dimensional spaces, facilitating processes such as molecule generation or material synthesis (Bilodeau et al., 2022; Zeni et al., 2023). However, simply approximating the data distribution is insufficient for real-world discovery, where exploration beyond high (data) density regions is essential.

Nonetheless, as illustrated in Fig. 1, these models excel at capturing complex data manifolds that are often significantly lower-dimensional than the ambient space (Stanczuk et al., 2024; Kamkari et al., 2024; Chen et al., 2023), and can synthesize realistic novel samples that satisfy intricate constraints (e.g., valid drug molecules or materials). Yet, when the goal shifts to exploring novel regions within that manifold, a fundamental question remains:

How can we leverage the representational power of generative models to guide exploration?

Our approach In this work, we tackle this challenge by first introducing the *maximum entropy manifold exploration* problem (Section 3). This involves learning a continuous-time reinforcement

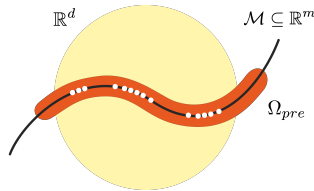


Figure 1: A diffusion model π^{pre} pre-trained on a set of points (white) implicitly learns a set Ω_{pre} (orange) approximating the true low-dimensional data manifold $\mathcal{M} \subseteq \mathbb{R}^m$ (black) with $m \ll d$. The approximate data manifold Ω_{pre} can be significantly smaller than \mathbb{R}^d (yellow).

[†] Indicates equal contribution. Corresponding author is Riccardo De Santi at <rdesanti@ethz.ch>.

learning policy (Doya, 2000; Zhao et al., 2024) that governs a new diffusion model to optimally explore the approximate data manifold implicitly captured by a pre-trained model. To this end, we present a theoretically grounded algorithmic principle that enables self-guided exploration via a diffusion model’s own representational power of the density it induces (Section 4). This turns exploration into density estimation, a task well-known to be challenging in high-dimensional real-world settings (Song et al., 2020; Kingma et al., 2021; Skreta et al., 2024). To overcome this obstacle and render the method proposed truly scalable, we leverage a fundamental connection between the entropy of the density induced by a diffusion model and its score function. Building on this, we propose a practical algorithm that performs manifold exploration through sequential fine-tuning of the pre-trained model (Section 6). We provide theoretical convergence guarantees for optimal exploration in a simplified illustrative setting by interpreting the algorithm proposed as a mirror descent scheme (Nemirovskij & Yudin, 1983; Lu et al., 2018) (Section 5), and then generalize the analysis to realistic settings building on recent understanding of mirror flows (Hsieh et al., 2019) (Section 7). Finally, we provide an experimental evaluation of the proposed method, demonstrating its practical relevance on both synthetic and high-dimensional image data, where we leverage a pre-trained text-to-image diffusion model (Section 8).

Our contributions To sum up, in this work we present the following contributions:

- The maximum entropy manifold exploration problem, that captures the goal of exploration over the approximate data manifold implicitly represented by a pre-trained diffusion model (Section 3)
- A scalable algorithmic principle for manifold exploration that leverages the representational power of a pre-trained diffusion model (Section 4), and a theoretically grounded algorithm based on sequential fine-tuning (Section 6).
- Convergence guarantees for the algorithm presented both under simplified and realistic assumptions leveraging recent understanding of mirror flows (Sections 5 and 7).
- An experimental evaluation of the proposed method showcasing its practical relevance on both an illustrative task and a high-dimensional text-to-image setting (Section 8).

2 BACKGROUND AND NOTATION

General Notation. We denote with $\mathcal{X} \subseteq \mathbb{R}^d$ an arbitrary set. Then, we indicate the set of Borel probability measures on \mathcal{X} with $\mathbb{P}(\mathcal{X})$, and the set of functionals over the set of probability measures $\mathbb{P}(\mathcal{X})$ as $\mathbb{F}(\mathcal{X})$. We write $d\mu = \rho dx$ to express that the density function of $\mu \in \mathbb{P}(\mathcal{X})$ with respect to the Lebesgue measure is ρ . Along this work, all integrals without an explicit measure are interpreted w.r.t. the Lebesgue measure. Given an integer N , we define $[N] := \{1, \dots, N\}$. Moreover, for two densities $\mu, \nu \in \mathbb{P}(\mathcal{X})$, we denote with $D_{KL}(\mu, \nu)$ the forward Kullback–Leibler divergence between μ and ν . Ultimately, we denote by $\mathcal{U}[0, a]$ the uniform density over the bounded set $[0, a]$ with $a \in \mathbb{R}_+$.

Continuous-time diffusion models. Diffusion models (DMs) are deep generative models that approximately sample a complex data distribution by learning from observations a dynamical system to map noise to novel valid data points (Song & Ermon, 2019). First, we introduce a forward stochastic differential equation (SDE) transforming to noise data points sampled from the data distribution p_{data} :

$$dX_t = f(X_t, t)dt + g(t)dB_t \text{ with } X_0 \sim p_{data} \quad (1)$$

where $X_t \in \mathbb{R}^d$ represents a d -dimensional point, $(B_t, t \geq 0)$ is d -dimensional Brownian motion, $f : \mathbb{R}_+ \times \mathbb{R}^d \rightarrow \mathbb{R}^d$ is a drift coefficient, and $g : \mathbb{R}_+ \rightarrow \mathbb{R}_+$ is a diffusion coefficient. We denote with p_t the marginal density at time t . Given a time horizon $t > 0$, one can sample $X_t \sim p_t$ by running the forward SDE in Eq. (1). We denote the time-reversal process by $X_t^{rev} := X_{T-t}$ for $0 \leq t \leq T$, following the backward SDE:

$$dX_t^{rev} = f^{rev}(X_t^{rev}, T-t)dt + \eta g(T-t)dB_t \quad (2)$$

with $f^{rev}(X_t^{rev}, T-t)$ corresponding to $-f(X_t^{rev}, T-t) + \frac{1+\eta^2}{2}g^2(T-t)\nabla_x \log p_{T-t}(X_t^{rev})$, where $\nabla_x \log p_t(x)$ is the score function, and $\eta \in [0, 1]$. By following the backward SDE in Eq. (2) from $X_T \sim p_T$, after T steps one obtains $X_0 = X_T^{rev} \sim p_0 = p_{data}$. In practice, p_T is replaced by a data-independent noise distribution $p_\infty \approx p_T$ for large T , typically a Gaussian¹ (Tang & Zhao, 2024).

Score matching and generation. Since the score function $\nabla_x \log p_t(x)$ is unknown, it is typically approximated by a neural network $s_\theta(x, t)$ learned by minimizing the MSE at points sampled according to the forward process, namely $\mathcal{J}(\theta) := \mathbb{E}_{t \sim \mathcal{U}[0, T]} \mathbb{E}_{x \sim p_t} [\omega(t) \|s_\theta(x, t) - \nabla_x \log p_t(x)\|_2^2]$,

¹In the following, we will choose p_∞ to be a truncated Gaussian for the sake of theoretical analysis.

where $\omega : [0, T] \rightarrow \mathbb{R}_{>0}$ is a weighting function. Crucially, this is equivalent to the denoising score matching objective (Vincent, 2011) consisting in estimating a minimizer θ^* of:

$$\mathbb{E}_{t \sim \mathcal{U}[0, T]} \omega(t) \mathbb{E}_{x_0 \sim p_0} \mathbb{E}_{x_t | x_0} \|s_\theta(x, t) - \nabla_{x_t} \log p_t(x_t | x_0)\|_2^2$$

where $p_t(\cdot | x_0)$ is the conditional distribution of x_t given an initial sample $x_0 \sim p_0$, which has a closed-form for typical diffusion dynamics. Once an approximate score function s_{θ^*} is learned, it can generate novel points approximately sampled from the data distribution. This is achieved by sampling an initial noise sample $X_0^{\leftarrow} \sim p_\infty$ and following the backward SDE in Eq. (2), replacing the true score $\nabla_x \log p_t(x)$ with s_{θ^*} , leading to the process $\{X_t^{\leftarrow}\}_{t \in [0, T]}$. Next, we introduce a framework that we will leverage to fine-tune a pre-trained diffusion model.

Continuous-time reinforcement learning. We formulate finite-horizon continuous-time reinforcement learning (RL) as a specific class of stochastic control problems (Wang et al., 2020; Jia & Zhou, 2022; Zhao et al., 2024). Given a state space \mathcal{X} and an action space \mathcal{A} , we consider the transition dynamics governed by the following diffusion process, where we invert the direction of the time variable:

$$d\bar{X}_t = b(\bar{X}_t, t, a_t)dt + \sigma(t)dB_t \text{ with } \bar{X}_0 \sim \mu \quad (3)$$

where $\mu \in \mathbb{P}(\mathcal{X})$ is an initial state distribution, $(B_t, t \geq 0)$ is d -dimensional Brownian motion, $b : \mathcal{X} \times \mathcal{A} \rightarrow \mathbb{R}^d$ is the drift coefficient, $\sigma : [0, T] \rightarrow \mathbb{R}_+$ is the diffusion coefficient, and $a_t \in \mathcal{A}$ is a selected action. In the following, we consider a state space $\mathcal{X} := \mathbb{R}^d \times [0, T]$, and denote by (Markovian) policy a function $\pi(X_t, t) \in \mathbb{P}(\mathcal{A})$ mapping a state $(x, t) \in \mathcal{X}$ to a density over the action space \mathcal{A} , and denote with p_t^π the marginal density at time t induced by policy π . In particular, we will consider deterministic policies so that $a_t = \pi(X_t, t)$.

Pre-trained diffusion model as an RL policy. A pre-trained diffusion model with score function s^{pre} can be interpreted as an action process $a_t^{pre} := s^{pre}(X_t^{\leftarrow}, T - t)$, where a_t^{pre} is sampled from a continuous-time RL policy $a_t^{pre} \sim \pi^{pre}$. As a consequence, we can express the backward SDE induced by the pre-trained score s^{pre} as follows:

$$dX_t^{\leftarrow} = b(X_t^{\leftarrow}, t, a_t^{pre})dt + \eta\sigma(t)dB_t \quad (4)$$

where we define $b(x, t, a) := -f(x, T - t) + \frac{1+\eta^2}{2}g^2(T - t) \cdot a$ and $\sigma(t) = g(T - t)$ (Zhao et al., 2024). In the following, we denote the pre-trained diffusion model by its (implicit) policy π^{pre} , which induces a marginal density $p_T^{pre} := p_T^{\pi^{pre}}$ approximating the data distribution p_{data} .

3 PROBLEM SETTING: MAXIMUM ENTROPY MANIFOLD EXPLORATION

We aim to fine-tune a pre-trained diffusion model π^{pre} to obtain a new model π^* , inducing a process:

$$d\bar{X}_t = b(\bar{X}_t, t, a_t^*)dt + \eta\sigma(t)dB_t \text{ with } a_t^* \sim \pi_t^* \quad (5)$$

that rather than imitating the data distribution p_{data} aims to induce a marginal state distribution $p_T^{\pi^*}$ that maximally explores the *approximate data manifold* Ω_{pre} defined as:

$$\Omega_{pre} = \text{supp}(p_T^{pre}) \quad (6)$$

Formally, we pose the exploration problem as optimization of an entropy functional over the space of marginal distributions p_T^π supported over the approximate data manifold. Crucially, Ω_{pre} , which is typically a complex set, e.g., a molecular space, is defined only implicitly via the pre-trained diffusion model π^{pre} as expressed in Eq. (6). Formally, we state the exploration problem as follows.

Maximum Entropy Manifold Exploration

$$\begin{aligned} \arg \max_{\pi} \quad & \mathcal{H}(p_T^\pi) \\ \text{s.t.} \quad & p_T^\pi \in \mathbb{P}(\Omega_{pre}) \end{aligned} \quad (7)$$

Here, $\mathcal{H} \in \mathbb{F}(\Omega_{pre})$ denotes the differential entropy quantifying exploration, expressed as:

$$\mathcal{H}(\mu) = - \int d\mu \log \frac{d\mu}{dx}, \quad \mu \in \mathbb{P}(\Omega_{pre}) \quad (8)$$

For this objective to be well defined, i.e., the maximum is achieved by some measure $\mu \in \mathbb{P}(\Omega_{pre})$, a sufficient condition is stated in the following and proved in Apx. C.

Proposition 1 (Ω_{pre} is compact). *Suppose that s^{pre} is Lipschitz and the noise distribution p_0 is the truncated Gaussian. Then Ω_{pre} spanned by an ODE sampler (i.e., Eq.(5) with $\eta = 0$) is compact.*

Notice that these assumptions are standard for analysis of diffusion processes, (e.g., Lee et al., 2022; Pidstrigach, 2022), and not limiting in practice. Proposition 1 implies that Ω_{pre} is a bounded subset of \mathbb{R}^d , which according to the manifold hypothesis approximates a lower-dimensional data manifold (Li et al., 2024; Chen et al., 2023; Stanczuk et al., 2024; Kamkari et al., 2024), as illustrated in Fig. 1. Crucially, both the constraint set $\mathbb{P}(\Omega_{pre})$ and the marginal density p_T^π in Problem 7 are *never represented explicitly*, but only implicitly as functions of the pre-trained policy π^{pre} and of the new policy π respectively. In the rest of this work, we show that Problem (7) can be solved by fine-tuning the initial pre-trained model w.r.t. rewards obtained by sequentially linearizing the entropy functional. Towards this goal, in the next section, we introduce a scalable algorithmic principle that guides exploration by leveraging the representational capacity of the pre-trained diffusion model.

4 A PRINCIPLE FOR SCALABLE EXPLORATION

Towards tackling the maximum entropy manifold exploration problem in Eq. (7), we first introduce a principle for exploration corresponding to a specific (intrinsic) reward function for fine-tuning. To this end, we define the first variation of a functional over a space of probability measures Hsieh et al. (2019). A functional $\mathcal{F} \in \mathbb{F}(\mathcal{X})$, where $\mathcal{F} : \mathbb{P}(\mathcal{X}) \rightarrow \mathbb{R}$, has first variation at $\mu \in \mathbb{P}(\mathcal{X})$ if there exists a function $\delta\mathcal{F}(\mu) \in \mathbb{F}(\mathcal{X})$ such that for all $\mu' \in \mathbb{P}(\mathcal{X})$ it holds that:

$$\mathcal{F}(\mu + \epsilon\mu') = \mathcal{F}(\mu) + \epsilon\langle\mu', \delta\mathcal{F}(\mu)\rangle + o(\epsilon).$$

where the inner product is interpreted as an expectation. We can now present the following exploration principle as KL-regularized maximization of the entropy first variation evaluated at p_T^{pre} .

Regularized Entropy First Variation Maximization

$$\arg \max_{\pi} \langle \delta\mathcal{H}(p_T^{pre}), p_T^\pi \rangle - \alpha D_{KL}(p_T^\pi, p_T^{pre}) \quad (9)$$

4.1 GENERATIVE EXPLORATION VIA DENSITY ESTIMATION

Crucially, this algorithmic principle does not rely on explicit uncertainty quantification and uses the generative model’s ability to represent the density p_T^{pre} to direct exploration. By introducing a function $f : \mathcal{X} \rightarrow \mathbb{R}$ defined for all $x \in \mathcal{X}$ as:

$$f(x) := \delta\mathcal{H}(p_T^{pre})(x) = -\log(p_T^{pre})(x) \quad (10)$$

the exploration principle in Eq. (9) computes a policy π^* inducing $p_T^{\pi^*}$ with high density in regions where p_T^{pre} has low density due to limited pre-training samples. Moreover, the KL regularization in Eq. (9) implicitly enforces $p_T^{\pi^*}$ to lie on the approximate data manifold Ω_{pre} . Formally, we have that:

$$\Omega_{\pi^*} := \text{supp}(p_T^{\pi^*}) \subseteq \text{supp}(p_T^{pre}) = \Omega_{pre} \quad \forall \alpha > 0 \quad (11)$$

4.2 EASY TO OPTIMIZE, BUT HARD TO ESTIMATE DENSITY

Existing fine-tuning methods for diffusion models can only optimize linear functionals of p_T^π , namely $\mathcal{L}(\mu) = \langle f, \mu \rangle \in \mathbb{F}(\mathcal{X})$, since they can be represented as classic (reward) functions $f : \mathcal{X} \rightarrow \mathbb{R}$, defined over the design space \mathcal{X} , e.g., space of molecules. Although the entropy functional \mathcal{H} in Eq. (7) is non-linear w.r.t. p_T^π , its first variation is a linear functional. As a consequence, by rewriting it as shown in Eq. (10), it can be optimized using existing fine-tuning methods for classic reward functions via stochastic optimal control schemes (e.g., Uehara et al., 2024b; Domingo-Enrich et al., 2024; Zhao et al., 2024), where the fine-tuning objective is:

$$\pi^* \in \arg \max_{\pi} \mathbb{E}_{x \sim \pi} \left[-\log(p_T^{pre})(x) \right] - \alpha D_{KL}(p_T^\pi, p_T^{pre})$$

We have shown that exploration can be self-guided by a generative model using its representational power of the density it induces. But unfortunately, estimating p_T^{pre} is well-known to be a challenging task in real-world high-dim. settings (Song et al., 2020; Kingma et al., 2021; Skreta et al., 2024).

4.3 GENERATIVE EXPLORATION WITHOUT DENSITY ESTIMATION

In the following, we show that in the case of diffusion models, the entropy’s first variation at the marginal density p_T^π induced by π , as in Eq. (10) with $\pi = \pi^{pre}$, can be optimized fully bypassing density estimation. This can be achieved by leveraging the following fundamental connection between the gradient of the entropy first variation $\nabla_x \delta \mathcal{H}(p_T^\pi)$ and the score $s^\pi(\cdot, T)$.

Gradient of entropy first variation = Negative score

$$\nabla_x \delta \mathcal{H}(p_T^\pi) = -\nabla_x \log p_T^\pi \simeq -s^\pi(\cdot, T) \quad (12)$$

Using Eq. (12), it is possible to solve the maximization problem in Eq. (9) by leveraging a first-order fine-tuning method such as Adjoint Matching Domingo-Enrich et al. (2024) with $\nabla_x f(x) := -s^{pre}(x, T)$ as reward gradient, where s^{pre} is the known (neural) score model approximating the true score function. This realization overcomes the limitation of density estimation and renders the method scalable for high-dimensional real-world problems. For the sake of completeness, we report a detailed pseudocode of its implementation in Appendix F.

4.4 BEYOND MAXIMUM ENTROPY EXPLORATION

As shown in Sec. 8, beyond the goal of maximum (entropy) exploration, the principle in Eq. (9) can be used to achieve the desired trade-off between exploration and validity by controlling the regularization coefficient α . Higher α values lead to a fine-tuned model π that conservatively aligns with the validity encoded in the pre-trained model π^{pre} . In contrast, low α values enable exploration of low density regions within the approximate data manifold Ω_{pre} . The latter modality is particularly relevant when a validity checker is available, e.g., synthetic accessibility (SA) scores for molecules (Ertl & Schuffenhauer, 2009), or formal verifiers for logic circuits (Coudert & Madre, 1990), allowing the discovery of new valid designs that expand the current manifold or dataset, effectively performing a guided data augmentation process (Zheng et al., 2023). In particular, one might wonder if there exists a value of α such that the obtained fine-tuned model can provably solve the maximum entropy exploration problem in Eq. (7). In the following section, we present a theoretical framework that answers this question positively under idealized assumptions.

5 PROVABLY OPTIMAL EXPLORATION IN ONE STEP

In this section, we show that under the assumptions of exact optimization and estimation of $\delta \mathcal{H}(p_T^{pre})$, a single fine-tuning step using Eq. (9) yields an optimally explorative policy π for entropy maximization over Ω_{pre} . First, recall the notion of Bregman divergence induced by a functional $\mathcal{Q} \in \mathbb{F}(\mathcal{X})$ between two densities $\mu, \nu \in \mathbb{P}(\mathcal{X})$, namely $D_{\mathcal{Q}}(\mu, \nu) := \mathcal{Q}(\mu) - \mathcal{Q}(\nu) - \langle \delta \mathcal{Q}(\nu), \mu - \nu \rangle$. In the following, we view the principle in Eq. (9) as a step of mirror descent (Nemirovskij & Yudin, 1983) and the KL divergence term as the Bregman divergence induced by an entropic mirror map $\mathcal{Q} = \mathcal{H}$, i.e., $D_{KL}(\mu, \nu) = D_{\mathcal{H}}(\mu, \nu)$. We can now state the following lemma regarding $\mathcal{F} = \mathcal{H}$ based on the notions of relative smoothness and strong convexity presented in Definition 1.

Lemma 5.1 (Relative smoothness and strong convexity for $\mathcal{F} = \mathcal{Q} = \mathcal{H}$). *For $\mathcal{F} = \mathcal{Q} = \mathcal{H}$ as in Eq. (9), we have that \mathcal{F} is 1-smooth (i.e., $L = 1$) and 1-strongly convex (i.e., $l = 1$) relative to \mathcal{Q} .*

We can now state the following idealized assumptions as well as the one-step convergence guarantee.

Assumption 5.1 (Exact estimation and solver). *Consider the following assumptions: (i) Exact score estimation: $s^{pre}(\cdot, T) = \nabla_x \log p_T^{pre}$, and (ii) The optimization problem in Eq. (9) is solved exactly.*

Theorem 5.2 (One-step convergence). *Given Assumptions 5.1, fine-tuning a pre-trained model π^{pre} according to Eq. (9) with $\alpha = L = 1$, leads to a policy π inducing a marginal distribution $p_T^\pi \in \mathbb{P}(\Omega_{pre})$ such that:*

$$\mathcal{H}(p_T^*) - \mathcal{H}(p_T^\pi) \leq \frac{L-l}{K} D_{KL}(p_T^*, p_T^{pre}) = 0 \quad (13)$$

where $p_T^* := p_T^{\pi^*}$ is the optimal marginal density induced by $\pi^* \in \arg \max_{\pi \in \Lambda} \mathcal{H}(p_T^\pi)$ with $\Lambda = \{\pi : p_T^\pi \in \mathbb{P}(\Omega_{pre})\}$ being the set of policies compatible with the approximate data manifold Ω_{pre} .

Theorem 5.2 suggest promising performance when using Eq. (9) as a fine-tuning objective for maximum entropy exploration, as under Assumptions 5.1, it yields an optimally explorative policy in

one step. However, Assumptions 5.1 rarely hold in practice since the score $s^{pre}(\cdot, T)$ is approximately learned from data, and solving Eq. (9) relies on approximate high-dimensional stochastic control methods. Thus, optimizing the entropy first variation is actually unlikely to lead to an optimally explorative diffusion model in one step, as shown experimentally in Sec. 8. To address this, in the next section we propose an exploration algorithm by building on the principle in Eq. (9).

6 SCORE-BASED MAXIMUM ENTROPY MANIFOLD EXPLORATION

In the following, we present **Score-based Maximum Entropy Manifold Exploration (S-MEME)**, see Algorithm 1, which reduces manifold exploration to sequential fine-tuning of the pre-trained diffusion model π^{pre} by following a mirror descent (MD) scheme (Nemirovskij & Yudin, 1983). Crucially, each iteration k of S-MEME corresponds to a fine-tuning step according to Equation (9), where the pre-trained model $\pi^{pre} =: \pi_0$ is then replaced by the model at the previous iteration, namely π_{k-1} . Concretely, this makes it possible to reduce the optimization of the entropy functional, which is non-linear w.r.t. p_T^π , to a sequence of optimization problems of linear functionals.

Algorithm 1 Score-based Maximum Entropy Manifold Exploration (S-MEME)

- 1: **input:** K : number of iterations, π^{pre} : pre-trained diffusion, $\{\alpha_k\}_{k=1}^K$ regularization coefficients
 - 2: **init:** $\pi_0 := \pi^{pre}$
 - 3: **for** $k = 1, 2, \dots, K$ **do**
 - 4: **Set:** $\nabla_x f_k = -s^{k-1}$ with $s^{k-1} = s^{\pi_{k-1}}$
 - 5: **Compute** π_k via first-order linear fine-tuning:

$$\pi_k \leftarrow \text{LINEARFINETUNINGSOLVER}(\nabla_x f_k, \alpha_k, \pi_{k-1})$$
 - 6: **end for**
 - 7: **output** policy $\pi := \pi_K$
-

Algorithm 1 requires as inputs a pre-trained diffusion model π^{pre} , the number of iterations K , and a schedule of regularization coefficients $\{\alpha_k\}_{k=1}^K$. At each iteration, S-MEME sets the gradient of the entropy first variation evaluated at the previous policy π_{k-1} , namely $\nabla_x \delta \mathcal{H}(p_T^{k-1})$, to be the score $s^{k-1} := s^{\pi_{k-1}}$ associated to the diffusion model π_{k-1} obtained at the previous iteration (line 3). Then, it computes policy π_k by solving the following fine-tuning problem

$$\arg \max_{\pi} \mathbb{E}_{x \sim \pi} \left[-\log(p_T^{k-1})(x) \right] - \alpha_k KL(p_T^\pi, p_T^{k-1})$$

via a first-order solver such as Adjoint Matching (Domingo-Enrich et al., 2024), using $\nabla f_k := -s^{k-1}(\cdot, T)$ as in Eq. (12) (line 4). Ultimately, it returns a final policy $\pi := \pi_K$. We report a possible implementation of LINEARFINETUNINGSOLVER in Appendix F.

Crucially, S-MEME controls the distributional behavior of the final diffusion model π , which is essential to optimize the entropy as it is a non-linear functional over $\mathbb{P}(\Omega_{pre})$. However, it is still unclear whether the algorithm provably converges to the optimally explorative diffusion model π^* . In the next section, we answer affirmatively this question by developing a theoretical analysis under general assumptions based on recent results for mirror flows (Hsieh et al., 2019).

7 MANIFOLD EXPLORATION GUARANTEES

The purpose of this section is to establish a realistic framework under which Algorithm 1 is guaranteed to solve the maximum entropy manifold exploration Problem (7).

First, we present the needed assumptions and provide an explanation of why they are realistic. Conceptually, these align with the *stochastic approximation* framework of Benaïm (2006); Mertikopoulos et al. (2024); Hsieh et al. (2021). Specifically, recall that $p_T^k := p_T^{\pi_k}$ represents the (stochastic) density produced by the LINEARFINETUNINGSOLVER oracle at the k -th step of S-MEME, and consider the following *mirror descent* iterates, where $1/\lambda_k = \alpha_k$ in Algorithm 1:

$$p_{\#}^k := \arg \max_{p \in \mathbb{P}(\Omega_{pre})} \langle d\mathcal{H}(p_T^{\pi_{k-1}}), p \rangle - \frac{1}{\gamma_k} D_{KL}(p, p_T^{\pi_{k-1}}) \quad (\text{MD}_k)$$

As explained in Section 5, the maximum entropy manifold exploration problem (7) can be solved in a single step using (MD_k) . However, in realistic settings where only noisy *and* biased approximations of

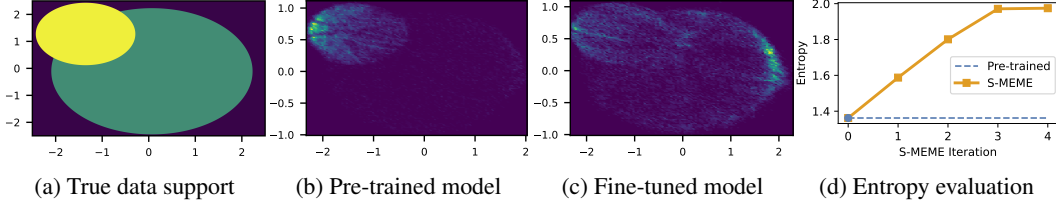


Figure 2: Illustrative example with unbalanced pre-trained model π^{pre} . (2a) Support of true data distribution composed of high-density (yellow) and low-density (green) regions. (2b) Sample from pre-trained model π^{pre} . (2c) Sample from π_4 obtained after 4 steps of S-MEME. (2d) Entropy estimation of densities $\{p_k\}_{k=1}^K$. Notice that S-MEME returns a fine-tuned model with significantly higher entropy than π^{pre} (see 2c and 2d), and higher density in low-density regions for the pre-trained model (compare (2a) and (2c)), while preserving the data support shown in 2a.

(MD_k) are available, it becomes essential to quantify the deviations due to these approximations from the idealized iterates in (MD_k). Additionally, the step sizes γ_k must be carefully designed to account for such deviations. This section aims to achieve precisely this goal. To this end, we first require:

Assumption 7.1 (Support Compatibility). *We assume that $\text{supp}(p_T^{\pi_k}) \subseteq \text{supp}(p_{pre})$ for all k .*

Next, we require a purely technical assumption that is typically satisfied in practice:

Assumption 7.2. *The sequence $\{\delta\mathcal{H}(p_T^{\pi_k})\}_k$ is precompact in the topology induced by the L_∞ norm.*

Now, denote by \mathcal{G}_k the filtration up to step k , and consider the decomposition of the oracle into its *noise* and *bias* parts:

$$b_k := \mathbb{E} [\delta\mathcal{H}(p_T^{\pi_k}) - \delta\mathcal{H}(p_\#^k) | \mathcal{G}_k], \quad U_k := \delta\mathcal{H}(p_T^{\pi_k}) - \delta\mathcal{H}(p_\#^k) - b_k \quad (14)$$

Conditioned on \mathcal{G}_k , U_k has zero mean, while b_k captures the *systematic* error. We then assume:

Assumption 7.3 (Noise and Bias). *The following events happen almost surely:*

$$\|b_k\|_\infty \rightarrow 0 \quad (15)$$

$$\sum_k \mathbb{E} \left[\gamma_k^2 \left(\|b_k\|_\infty^2 + \|U_k\|_\infty^2 \right) \right] < \infty \quad (16)$$

$$\sum_k \gamma_k \|b_k\|_\infty < \infty \quad (17)$$

Two important remarks are worth noting. First, (15) is a necessary condition for convergence — violating it allows for counterexamples where no algorithm can solve the maximum entropy problem. Second, (16) and (17) capture the trade-off between the accuracy of `LINEARFINETUNINGSOLVER` and step size aggressiveness, γ_k . Intuitively, a smaller noise and bias allows for the use of larger step sizes. Concretely, (16) and (17) ensure that finding the optimally explorative policy succeeds with probability 1. We are now finally ready to state the following result.

Theorem 7.1 (Convergence under general assumptions). *Consider the standard Robbins-Monro step-size rule: $\sum_k \gamma_k = \infty$, $\sum_k \gamma_k^2 < \infty$. Then under Assumptions 7.3, the sequence of marginal densities p_T^k induced by the iterates π_k of Algorithm 1 converges weakly to p_T^* almost surely. Formally, we have that:*

$$p_T^k \rightharpoonup p_T^* \quad a.s. \quad (18)$$

where $p_T^* \in \arg \max_{p_T \in \mathbb{P}(\Omega_{pre})} \mathcal{H}(p_T)$ is the maximum entropy density compatible with Ω_{pre} .

8 EXPERIMENTAL EVALUATION

In this section, we analyze the ability of S-MEME to induce explorative policies on two tasks: (1) An illustrative example to visually show exploration and ability to sample from low-density regions (see Fig. 2), and (2) A text-to-image task aiming to explore the approximate manifold of *creative architecture* designs (see Fig. 3). Additional details on experiments are provided in Appendix G.

(1) Illustrative setting. In this experiment, we consider the setting where the density p_T^{pre} induced by a pre-trained model π^{pre} has a high-density region (yellow area in Fig. 2a) and a low-density region (green area in in Fig. 2a). As illustrated in Fig. 2a, the pre-trained model π^{pre} induces an unbalanced



Figure 3: Generated images from π^{pre} (top) and π_3 (bottom) for a fixed set of initial noisy samples using the prompt "A creative architecture.". We observe an increase in complexity and originality of the S-MEME generated images while preserving semantic faithfulness, likely hinting at higher probability of sampling from a lower-density region of π^{pre} .

density, where $N = 80000$ samples are obtained mostly from the high-density area. For quantitative evaluation, we compute a Monte Carlo estimate of $\mathcal{H}(p_T^\pi)$. Fig. 2 shows that S-MEME can induce a highly explorative density in terms of entropy (see Fig. 2d) compared with the pre-trained model, after only $K = 4$ iterations. One can notice that the density induced by the fine-tuned model (see Fig. 2c) is significantly more uniform and higher in low-probability regions for the pre-trained model (see right region of Fig. 2c), while preserving the support of the data distribution.

(2) Text-to-image manifold exploration. We consider the problem of exploring the data manifold of *creative architecture* designs given a pre-trained text-to-image diffusion model. For this we utilize the stable diffusion (SD) 1.5 (Rombach et al., 2021) pre-trained on the LAION-5B dataset (Schuhmann et al., 2022). Since SD-1.5 uses classifier-free guidance (Ho & Salimans, 2022), we fine-tune the obtained velocity with guidance scale of $w = 8$, which is standard for SD-1.5. Similarly, we also use the same guidance scheme for the fine-tuned model. We fine-tuned the checkpoint with $K = 3$ iterations of S-MEME on a single Nvidia H100 GPU for the prompt "A creative architecture.". In Figure 3, we show images generated from π^{pre} , π_1 and π_3 , resulting from the same initial noise samples. One can notice an increase in the complexity and originality of the respective images, likely hinting at higher probability of the fine-tuned model to sample from a lower-density region for π^{pre} . Moreover, less conservative architectures are sampled with more steps of S-MEME while preserving semantic faithfulness. We measure this in Table 1 by computing the Fréchet inception distance (FID) (Heusel et al., 2017), the Gaussian cross-entropy in feature space of Inception-v3 between $p_T^{\pi^k}$ and p_T^{pre} for $k = 1, 2, 3$, as well as the CLIP score (Hessel et al., 2021). The main reason for these proxy metrics is the intractability of computing $\log p_T^{pre}(x)$ in high-dimensional spaces, such as that of images generated by a large diffusion model. One can notice from Table 1 an increase in FID and cross-entropy between the distributions as k increases, while the fine-tuned model preserves the CLIP score of the pre-trained model. We provide further results for text-to-image in Appendix H.

Table 1: FID, CLIP and cross-entropy eval. of p_T^{pre} and $p_T^{\pi^k}$. For $k = 1, 2, 3$, S-MEME achieves larger distance to p_T^{pre} while preserving high CLIP score.

	p_T^{pre}	S-MEME 1	S-MEME 2
FID	0.0	10.25	9.83
CLIP	22.27	20.79	20.88
$\hat{H}(p, p_T^{pre})$	-1916.47	564.72	482.81

9 CONCLUSION

This work tackles the fundamental challenge of leveraging the representational power of generative models for exploration. We first introduce a formal framework for exploration as entropy maximization over the approximate data manifold implicitly captured by a pre-trained diffusion model. Then, we present an algorithmic principle that guides exploration via density estimation, a challenging task in real-world settings. By exploiting a fundamental connection between entropy and a diffusion model’s score function, we overcome this problem and ensure scalability of the proposed principle for exploration. Building on this, we introduce S-MEME, a sequential fine-tuning algorithm that provably solves the exploration problem, with convergence guarantees grounded in recent advances in mirror flows. Finally, we validate the proposed method on both a conceptual benchmark and a high-dimensional text-to-image task, demonstrating its practical relevance.

ACKNOWLEDGEMENTS

This publication was made possible by the ETH AI Center doctoral fellowship to Riccardo De Santi, and postdoctoral fellowship to Marin Vlastelica. The project has received funding from the Swiss National Science Foundation under NCCR Catalysis grant number 180544 and NCCR Automation grant agreement 51NF40_180545.

REFERENCES

- Pierre-Cyril Aubin-Frankowski, Anna Korba, and Flavien Léger. Mirror descent with relative smoothness in measure spaces, with application to sinkhorn and em. *Advances in Neural Information Processing Systems*, 35:17263–17275, 2022.
- Michel Benaïm. Dynamics of stochastic approximation algorithms. In *Seminaire de probabilités XXXIII*, pp. 1–68. Springer, 2006.
- Michel Benaïm and Morris W Hirsch. Asymptotic pseudotrajectories and chain recurrent flows, with applications. *Journal of Dynamics and Differential Equations*, 8:141–176, 1996.
- Camille Bilodeau, Wengong Jin, Tommi Jaakkola, Regina Barzilay, and Klavs F Jensen. Generative models for molecular discovery: Recent advances and challenges. *Wiley Interdisciplinary Reviews: Computational Molecular Science*, 12(5):e1608, 2022.
- Minshuo Chen, Kaixuan Huang, Tuo Zhao, and Mengdi Wang. Score approximation, estimation and distribution recovery of diffusion models on low-dimensional data. In *International Conference on Machine Learning*, pp. 4672–4712. PMLR, 2023.
- Cheng Chi, Siyuan Feng, Yilun Du, Zhenjia Xu, Eric Cousineau, Benjamin Burchfiel, and Shuran Song. Diffusion policy: Visuomotor policy learning via action diffusion. *arXiv preprint arXiv:2303.04137*, 2023.
- Gabriele Corso, Hannes Stärk, Bowen Jing, Regina Barzilay, and Tommi Jaakkola. Diffdock: Diffusion steps, twists, and turns for molecular docking. *arXiv preprint arXiv:2210.01776*, 2022.
- Gabriele Corso, Yilun Xu, Valentin De Bortoli, Regina Barzilay, and Tommi Jaakkola. Particle guidance: non-iid diverse sampling with diffusion models. *arXiv preprint arXiv:2310.13102*, 2023.
- Olivier Coudert and Jean Christophe Madre. A unified framework for the formal verification of sequential circuits. In *The Best of ICCAD: 20 Years of Excellence in Computer-Aided Design*, pp. 39–50. Springer, 1990.
- Riccardo De Santi, Federico Arangath Joseph, Noah Liniger, Mirco Mutti, and Andreas Krause. Geometric active exploration in markov decision processes: the benefit of abstraction. *arXiv preprint arXiv:2407.13364*, 2024a.
- Riccardo De Santi, Manish Prajapat, and Andreas Krause. Global reinforcement learning: Beyond linear and convex rewards via submodular semi-gradient methods. *arXiv preprint arXiv:2407.09905*, 2024b.
- Carles Domingo-Enrich, Michal Drozdal, Brian Karrer, and Ricky TQ Chen. Adjoint matching: Fine-tuning flow and diffusion generative models with memoryless stochastic optimal control. *arXiv preprint arXiv:2409.08861*, 2024.
- Kenji Doya. Reinforcement learning in continuous time and space. *Neural computation*, 12(1): 219–245, 2000.
- Pavel Dvurechensky and Jia-Jie Zhu. Analysis of kernel mirror prox for measure optimization. In *International Conference on Artificial Intelligence and Statistics*, pp. 2350–2358. PMLR, 2024.
- Peter Ertl and Ansgar Schuffenhauer. Estimation of synthetic accessibility score of drug-like molecules based on molecular complexity and fragment contributions. *Journal of cheminformatics*, 1:1–11, 2009.

- Wendell H Fleming and Raymond W Rishel. *Deterministic and stochastic optimal control*, volume 1. Springer Science & Business Media, 2012.
- Zhaohan Daniel Guo, Mohammad Gheshlaghi Azar, Alaa Saade, Shantanu Thakoor, Bilal Piot, Bernardo Avila Pires, Michal Valko, Thomas Mesnard, Tor Lattimore, and Rémi Munos. Geometric entropic exploration. *arXiv preprint arXiv:2101.02055*, 2021.
- Paul R Halmos. *Measure theory*, volume 18. Springer, 2013.
- Elad Hazan, Sham Kakade, Karan Singh, and Abby Van Soest. Provably efficient maximum entropy exploration. In *International Conference on Machine Learning*, 2019.
- Jack Hessel, Ari Holtzman, Maxwell Forbes, Ronan Le Bras, and Yejin Choi. Clipscore: A reference-free evaluation metric for image captioning. In *Proceedings of the 2021 Conference on Empirical Methods in Natural Language Processing*, pp. 7514–7528, 2021.
- Martin Heusel, Hubert Ramsauer, Thomas Unterthiner, Bernhard Nessler, and Sepp Hochreiter. Gans trained by a two time-scale update rule converge to a local nash equilibrium. *Advances in neural information processing systems*, 30, 2017.
- Jean-Baptiste Hiriart-Urruty and Claude Lemaréchal. *Fundamentals of convex analysis*. Springer Science & Business Media, 2004.
- Jonathan Ho and Tim Salimans. Classifier-free diffusion guidance. *arXiv preprint arXiv:2207.12598*, 2022.
- Jonathan Ho, Ajay Jain, and Pieter Abbeel. Denoising diffusion probabilistic models. *Advances in neural information processing systems*, 33:6840–6851, 2020.
- Emiel Hooeboom, Victor Garcia Satorras, Clément Vignac, and Max Welling. Equivariant diffusion for molecule generation in 3d. In *International conference on machine learning*, pp. 8867–8887. PMLR, 2022.
- Ya-Ping Hsieh, Chen Liu, and Volkan Cevher. Finding mixed nash equilibria of generative adversarial networks. In *International Conference on Machine Learning*, pp. 2810–2819. PMLR, 2019.
- Ya-Ping Hsieh, Panayotis Mertikopoulos, and Volkan Cevher. The limits of min-max optimization algorithms: Convergence to spurious non-critical sets. In *International Conference on Machine Learning*, pp. 4337–4348. PMLR, 2021.
- Yanwei Jia and Xun Yu Zhou. Policy evaluation and temporal-difference learning in continuous time and space: A martingale approach. *Journal of Machine Learning Research*, 23(154):1–55, 2022.
- Hamidreza Kamkari, Brendan Leigh Ross, Rasa Hosseinzadeh, Jesse C Cresswell, and Gabriel Loaiza-Ganem. A geometric view of data complexity: Efficient local intrinsic dimension estimation with diffusion models. *arXiv preprint arXiv:2406.03537*, 2024.
- Mohammad Reza Karimi, Ya-Ping Hsieh, and Andreas Krause. Sinkhorn flow as mirror flow: A continuous-time framework for generalizing the sinkhorn algorithm. In *International Conference on Artificial Intelligence and Statistics*, pp. 4186–4194. PMLR, 2024.
- Diederik Kingma, Tim Salimans, Ben Poole, and Jonathan Ho. Variational diffusion models. *Advances in neural information processing systems*, 34:21696–21707, 2021.
- Michael Kirchhof, James Thornton, Pierre Ablin, Louis Béthune, Eugene Ndiaye, and Marco Cuturi. Sparse repellency for shielded generation in text-to-image diffusion models. *arXiv preprint arXiv:2410.06025*, 2024.
- Holden Lee, Jianfeng Lu, and Yixin Tan. Convergence for score-based generative modeling with polynomial complexity. *Advances in Neural Information Processing Systems*, 35:22870–22882, 2022.
- Lisa Lee, Benjamin Eysenbach, Emilio Parisotto, Eric Xing, Sergey Levine, and Ruslan Salakhutdinov. Efficient exploration via state marginal matching. *arXiv preprint arXiv:1906.05274*, 2019.

- Flavien Léger. A gradient descent perspective on sinkhorn. *Applied Mathematics & Optimization*, 84(2):1843–1855, 2021.
- Zihao Li, Hui Yuan, Kaixuan Huang, Chengzhuo Ni, Yinyu Ye, Minshuo Chen, and Mengdi Wang. Diffusion model for data-driven black-box optimization. *arXiv preprint arXiv:2403.13219*, 2024.
- David Lindner, Matteo Turchetta, Sebastian Tschiatschek, Kamil Ciosek, and Andreas Krause. Information directed reward learning for reinforcement learning. *Advances in Neural Information Processing Systems*, 34:3850–3862, 2021.
- Hao Liu and Pieter Abbeel. Behavior from the void: Unsupervised active pre-training. *Advances in Neural Information Processing Systems*, 34:18459–18473, 2021.
- Haihao Lu, Robert M Freund, and Yurii Nesterov. Relatively smooth convex optimization by first-order methods, and applications. *SIAM Journal on Optimization*, 28(1):333–354, 2018.
- Panayotis Mertikopoulos, Ya-Ping Hsieh, and Volkan Cevher. A unified stochastic approximation framework for learning in games. *Mathematical Programming*, 203(1):559–609, 2024.
- Zichen Miao, Jiang Wang, Ze Wang, Zhengyuan Yang, Lijuan Wang, Qiang Qiu, and Zicheng Liu. Training diffusion models towards diverse image generation with reinforcement learning. In *Proceedings of the IEEE/CVF Conference on Computer Vision and Pattern Recognition*, pp. 10844–10853, 2024.
- Mojmir Mutny, Tadeusz Janik, and Andreas Krause. Active exploration via experiment design in Markov chains. In *International Conference on Artificial Intelligence and Statistics*, 2023.
- Mirco Mutti, Lorenzo Pratissoli, and Marcello Restelli. Task-agnostic exploration via policy gradient of a non-parametric state entropy estimate. In *Proceedings of the AAAI Conference on Artificial Intelligence*, volume 35, pp. 9028–9036, 2021.
- Mirco Mutti, Riccardo De Santi, Piersilvio De Bartolomeis, and Marcello Restelli. Challenging common assumptions in convex reinforcement learning. *Advances in Neural Information Processing Systems*, 35:4489–4502, 2022a.
- Mirco Mutti, Riccardo De Santi, and Marcello Restelli. The importance of non-markovianity in maximum state entropy exploration. In *International Conference on Machine Learning*, pp. 16223–16239. PMLR, 2022b.
- Mirco Mutti, Riccardo De Santi, Piersilvio De Bartolomeis, and Marcello Restelli. Convex reinforcement learning in finite trials. *Journal of Machine Learning Research*, 24(250):1–42, 2023.
- Arkadij Semenovič Nemirovskij and David Borisovich Yudin. Problem complexity and method efficiency in optimization. 1983.
- Jakiw Pidstrigach. Score-based generative models detect manifolds. *Advances in Neural Information Processing Systems*, 35:35852–35865, 2022.
- Manish Prajapat, Mojmir Mutny, Melanie N Zeilinger, and Andreas Krause. Submodular reinforcement learning. *arXiv preprint arXiv:2307.13372*, 2023.
- Robin Rombach, Andreas Blattmann, Dominik Lorenz, Patrick Esser, and Björn Ommer. High-resolution image synthesis with latent diffusion models, 2021.
- Syedmorteza Sadat, Jakob Buhmann, Derek Bradley, Otmar Hilliges, and Romann M. Weber. Cads: Unleashing the diversity of diffusion models through condition-annealed sampling, 2024. URL <https://arxiv.org/abs/2310.17347>.
- Christoph Schuhmann, Romain Beaumont, Richard Vencu, Cade Gordon, Ross Wightman, Mehdi Cherti, Theo Coombes, Aarush Katta, Clayton Mullis, Mitchell Wortsman, et al. Laion-5b: An open large-scale dataset for training next generation image-text models. *Advances in Neural Information Processing Systems*, 35:25278–25294, 2022.

- Younggyo Seo, Lili Chen, Jinwoo Shin, Honglak Lee, Pieter Abbeel, and Kimin Lee. State entropy maximization with random encoders for efficient exploration. In *International Conference on Machine Learning*, pp. 9443–9454. PMLR, 2021.
- Marta Skreta, Lazar Atanackovic, Avishek Joey Bose, Alexander Tong, and Kirill Neklyudov. The superposition of diffusion models using the $\hat{\rho}$ density estimator. *arXiv preprint arXiv:2412.17762*, 2024.
- Jascha Sohl-Dickstein, Eric Weiss, Niru Maheswaranathan, and Surya Ganguli. Deep unsupervised learning using nonequilibrium thermodynamics. In *International conference on machine learning*, pp. 2256–2265. PMLR, 2015.
- Yang Song and Stefano Ermon. Generative modeling by estimating gradients of the data distribution. *Advances in neural information processing systems*, 32, 2019.
- Yang Song, Jascha Sohl-Dickstein, Diederik P Kingma, Abhishek Kumar, Stefano Ermon, and Ben Poole. Score-based generative modeling through stochastic differential equations. *arXiv preprint arXiv:2011.13456*, 2020.
- Jan Pawel Stanczuk, Georgios Batzolis, Teo Deveney, and Carola-Bibiane Schönlieb. Diffusion models encode the intrinsic dimension of data manifolds. In *Forty-first International Conference on Machine Learning*, 2024.
- Wenpin Tang. Fine-tuning of diffusion models via stochastic control: entropy regularization and beyond. *arXiv preprint arXiv:2403.06279*, 2024.
- Wenpin Tang and Hanyang Zhao. Contractive diffusion probabilistic models. *arXiv preprint arXiv:2401.13115*, 2024.
- Masatoshi Uehara, Yulai Zhao, Kevin Black, Ehsan Hajiramezanali, Gabriele Scalia, Nathaniel Lee Diamant, Alex M Tseng, Tommaso Biancalani, and Sergey Levine. Fine-tuning of continuous-time diffusion models as entropy-regularized control. *arXiv preprint arXiv:2402.15194*, 2024a.
- Masatoshi Uehara, Yulai Zhao, Kevin Black, Ehsan Hajiramezanali, Gabriele Scalia, Nathaniel Lee Diamant, Alex M Tseng, Sergey Levine, and Tommaso Biancalani. Feedback efficient online fine-tuning of diffusion models. *arXiv preprint arXiv:2402.16359*, 2024b.
- Soobin Um and Jong Chul Ye. Self-guided generation of minority samples using diffusion models. In *European Conference on Computer Vision*, pp. 414–430. Springer, 2025.
- Soobin Um, Suhyeon Lee, and Jong Chul Ye. Don’t play favorites: Minority guidance for diffusion models. *arXiv preprint arXiv:2301.12334*, 2023.
- Pascal Vincent. A connection between score matching and denoising autoencoders. *Neural computation*, 23(7):1661–1674, 2011.
- Haoran Wang, Thaleia Zariphopoulou, and Xun Yu Zhou. Reinforcement learning in continuous time and space: A stochastic control approach. *Journal of Machine Learning Research*, 21(198):1–34, 2020.
- Yuwei Yang, Zhenxing Wu, Xiaojun Yao, Yu Kang, Tingjun Hou, Chang-Yu Hsieh, and Huanxiang Liu. Exploring low-toxicity chemical space with deep learning for molecular generation. *Journal of Chemical Information and Modeling*, 62(13):3191–3199, 2022.
- Claudio Zeni, Robert Pinsler, Daniel Zügner, Andrew Fowler, Matthew Horton, Xiang Fu, Sasha Shysheya, Jonathan Crabbé, Lixin Sun, Jake Smith, et al. Mattergen: a generative model for inorganic materials design. *arXiv preprint arXiv:2312.03687*, 2023.
- Hanyang Zhao, Haoxian Chen, Ji Zhang, David D Yao, and Wenpin Tang. Scores as actions: a framework of fine-tuning diffusion models by continuous-time reinforcement learning. *arXiv preprint arXiv:2409.08400*, 2024.
- Chenyu Zheng, Guoqiang Wu, and Chongxuan Li. Toward understanding generative data augmentation. *Advances in neural information processing systems*, 36:54046–54060, 2023.

APPENDIX

A Related Work	14
B Definitions	16
C Proof for Proposition 1	17
D Proof for Section 5	18
E Proof for Section 7	19
E.1 Proof of Theorem 7.1	19
F Detailed Example of Algorithm Implementation	22
F.1 Pseudocode for implementation of Eq. (9)	22
G Experiment Details	23
H Additional Text-to-Image Results	23

A RELATED WORK

In the following, we present relevant work in related areas.

Maximum State Entropy Exploration. Maximum state entropy exploration, introduced by Hazan et al. (2019), addresses the pure-exploration RL problem of maximizing the entropy of the state distribution induced by a policy over a dynamical system’s state space (e.g., Lee et al., 2019; Mutti et al., 2021; Guo et al., 2021). The presented manifold exploration problem is closely related, with p_T^π representing the state distribution induced by policy π over a subset of the state space. Nonetheless, in Problem (7) the admissible state distributions $\mathbb{P}(\Omega_{pre})$ are represented only implicitly via a pre-trained generative model π^{pre} , able to capture complex design spaces, e.g., valid molecules. Moreover, exploration is guided by the diffusion model’s score function via Eq. 12, overcoming the need of explicit entropy or density estimation, a fundamental challenge in this area (Liu & Abbeel, 2021; Seo et al., 2021; Mutti et al., 2021). Recent studies have tackled maximum entropy exploration with finite sample budgets (e.g., Mutti et al., 2022b;a; 2023; Prajapat et al., 2023; De Santi et al., 2024b). We believe several ideas presented in this work can extend to such settings. Ultimately, to the best of our knowledge, this is the first work providing a rigorous theoretical analysis of maximum state entropy exploration over continuous state spaces, albeit for a specific sub-case, as well as leveraging this formulation for fine-tuning of diffusion models.

Continuous-time RL. Continuous-time RL extends stochastic optimal control (Fleming & Rishel, 2012) to handle unknown rewards or dynamics (e.g., Doya, 2000; Wang et al., 2020). Problem (7) represents the pure exploration case of continuous-time RL, where the goal is to compute a (purely) exploratory policy π over a subset of the state space $\Omega_{pre} \subseteq \mathcal{X}$ implicitly defined by a pre-trained generative model π^{pre} . Moreover, Problem (7) can be further motivated as a continuous-time RL reward learning setting (e.g., Lindner et al., 2021; Mutny et al., 2023; De Santi et al., 2024a), where an agent aims to learn an unknown homoscedastic reward function such as toxicity over a molecular space (Yang et al., 2022). To our knowledge, this is the first work that tackles maximum entropy exploration in a continuous-time RL setting.

Diffusion models fine-tuning via optimal control. Recent works have framed diffusion models fine-tuning with respect to a reward function $f : \mathcal{X} \rightarrow \mathbb{R}$ as an entropy-regularized stochastic optimal control problem (e.g., Uehara et al., 2024a; Tang, 2024; Uehara et al., 2024b; Domingo-Enrich et al., 2024). In this work, we introduce a scalable fine-tuning scheme, based on first-order solvers for classic rewards (e.g., Domingo-Enrich et al., 2024), that optimizes a broader class of functionals requiring information about the full density p_T^π , such as entropy and alternative exploration measures (De Santi et al., 2024b; Hazan et al., 2019). This paves the way to using diffusion models for optimization of distributional objectives, rather than simple scalar rewards. Beyond classic optimization, our framework is particularly relevant for Bayesian optimization, or bandit, problems (e.g., Uehara et al., 2024b), where the reward function to be optimized over the manifold is unknown and therefore exploration is essential.

Sample diversity in diffusion models generation. The lack of sample diversity in diffusion model generation is a key challenge tackled by various works (e.g., Corso et al., 2023; Um et al., 2023; Kirchhof et al., 2024; Sadat et al., 2024; Um & Ye, 2025). These methods complement ours by enabling diverse sampling from the fine-tuned explorative model obtained via S-MEME. While prior works focus on generating diverse samples from a fixed diffusion model, ours provides a framework for manifold exploration as policy optimization via reinforcement learning. This enables scalable and provable maximization of typical exploration measures in RL, such as state entropy (Hazan et al., 2019). Among related works, Miao et al. (2024) shares the closest intent, but lacks a formal setting with exploration guarantees, and the diffusion model’s exploration process relies on computing an external metric for exploration, rather than being self-guided via its own score function as S-MEME achieves via Eq. (12).

Optimization over probability measures via mirror flows. Recently, there has been a growing interest in analyzing optimization problems over spaces of probability measures. Existing works have explored applications including GANs Hsieh et al. (2019), optimal transport Aubin-Frankowski et al. (2022); Léger (2021); Karimi et al. (2024), and kernelized methods Dvurechensky & Zhu (2024). However, to the best of our knowledge, the case of the entropy-based objective in Problem 7, along with its associated relative smoothness analysis framework, has not been previously addressed. Moreover, prior approaches do not leverage a key aspect of our framework: the admissible space of probability measures, $\mathbb{P}(\Omega_{pre})$, is represented only implicitly via a pre-trained generative model, which can

approximate complex data manifolds learned from data, such as molecular spaces. This idea of optimization with implicit constraints captured by generative models is novel and absent in earlier work.

B DEFINITIONS

Definition 1 (Relative smoothness and relative strong convexity (Lu et al., 2018)). *Let $\mathcal{F} : \mathbb{P}(\mathcal{X}) \rightarrow \mathbb{R}$ a convex functional. We say that \mathcal{F} is L -smooth relative to $\mathcal{Q} \in \mathbb{F}(\mathcal{X})$ over $\mathbb{P}(\mathcal{X})$ if $\exists L$ scalar s.t. for all $\mu, \nu \in \mathbb{P}(\mathcal{X})$:*

$$\mathcal{F}(\nu) \leq \mathcal{F}(\mu) + \langle \delta \mathcal{F}(\mu), \nu - \mu \rangle + LD_{\mathcal{Q}}(\nu, \mu) \quad (19)$$

and we say that \mathcal{F} is l -strongly convex relative to $\mathcal{Q} \in \mathbb{F}(\mathcal{X})$ over $\mathbb{P}(\mathcal{X})$ if $\exists l \geq 0$ scalar s.t. for all $\mu, \nu \in \mathbb{P}(\mathcal{X})$:

$$\mathcal{F}(\nu) \geq \mathcal{F}(\mu) + \langle \delta \mathcal{F}(\mu), \nu - \mu \rangle + lD_{\mathcal{Q}}(\nu, \mu) \quad (20)$$

C PROOF FOR PROPOSITION 1

Recall the probability flow ODE in (Song et al., 2020, eq. (13)), which is what we use to generate p_T^{pre} (this is also a common practice in the literature). We know that the generative ODE corresponding to the backward SDE Equation (4) is written as (suppose $\eta = 1$ for simplicity)

$$dX_t^\leftarrow = \underbrace{-f(X_t^\leftarrow, T-t) + \frac{1}{2}g^2(T-t)s^{pre}(X_t^\leftarrow, T-t)}_{:=v(X_t^\leftarrow, t)} dt.$$

Here f is defined in the forward process Equation (1). Clearly the velocity field $v(x, t)$ is Lipschitz w.r.t. x due to the assumption that s^{pre} is Lipschitz and the fact that f is linear w.r.t. x . Consequently, *the flow map induced by the above ODE is Lipschitz*. As a result, since X_0 is sampled from a truncated Gaussian distribution which has a compact support, $\Omega^{pre} = \text{supp}(p_T^{pre})$ is also compact for any finite T .

D PROOF FOR SECTION 5

Theorem 5.2 (One-step convergence). *Given Assumptions 5.1, fine-tuning a pre-trained model π^{pre} according to Eq. (9) with $\alpha = L = 1$, leads to a policy π inducing a marginal distribution $p_T^\pi \in \mathbb{P}(\Omega_{pre})$ such that:*

$$\mathcal{H}(p_T^*) - \mathcal{H}(p_T^\pi) \leq \frac{L-l}{K} D_{KL}(p_T^*, p_T^{pre}) = 0 \quad (13)$$

where $p_T^* := p_T^{\pi^*}$ is the optimal marginal density induced by $\pi^* \in \arg \max_{\pi \in \Lambda} \mathcal{H}(p_T^\pi)$ with $\Lambda = \{\pi : p_T^\pi \in \mathbb{P}(\Omega_{pre})\}$ being the set of policies compatible with the approximate data manifold Ω_{pre} .

Proof. Towards proving this result, we interpret Eq. (9) as the first iteration of Algorithm 1. Hence, to prove the statement, it is sufficient to show that Algorithm 1 after one iteration computes π_1 inducing density $p_T^{\pi_1}$ such that $\mathcal{H}(p_T^*) = \mathcal{H}(p_T^{\pi_1})$. We prove this result by leveraging the properties of relative smoothness and relative strong convexity introduced in Sec. 5.

The analysis is based on a classic analysis for mirror descent via relative properties (Lu et al., 2018). First, we show the following, where for the sake of using a simple notation, we denote $p_T^{\pi_k}$ by μ_k , and consider an arbitrary density $\mu \in \mathbb{P}(\Omega_{pre})$.

$$\mathcal{H}(\mu_k) \leq \mathcal{H}(\mu_{k-1}) + \langle \delta \mathcal{H}(\mu_{k-1}), \mu_k - \mu_{k-1} \rangle + LD_{\mathcal{Q}}(\mu_k, \mu_{k-1}) \quad (21)$$

$$\leq \mathcal{H}(\mu_{k-1}) + \langle \delta \mathcal{H}(\mu_{k-1}), \mu - \mu_{k-1} \rangle + LD_{\mathcal{Q}}(\mu, \mu_{k-1}) - LD_{\mathcal{Q}}(\mu, \mu_k) \quad (22)$$

where in the first inequality we have used the L -smoothness of \mathcal{H} relative to $\mathcal{Q} = \mathcal{H}$ as in Definition 1, while in the last inequality we have used the three-point property of the Bregman divergence (Lu et al., 2018, Lemma 3.1) with $\phi(\mu) = \frac{1}{L} \langle \delta \mathcal{H}(\mu_{k-1}), \mu - \mu_{k-1} \rangle$, $z = \mu_{k-1}$, and $z^+ = \mu_k$. Then, we can derive:

$$\mathcal{H}(\mu_k) \leq \mathcal{H}(\mu) + (L - \mu) D_{\mathcal{Q}}(\mu, \mu_{k-1}) - LD_{\mathcal{Q}}(\mu, \mu_k) \quad (23)$$

by using the l -strong convexity of \mathcal{H} relative to $\mathcal{Q} = \mathcal{H}$ as in Definition 1. By induction, using monotonicity of the iterates and non-negativity of the Bregman divergence as in (Lu et al., 2018), one obtains:

$$\sum_{k=1}^K \left(\frac{L}{L-l} \right)^k (\mathcal{H}(\mu_k) - \mathcal{H}(\mu)) \leq LD_{\mathcal{Q}}(\mu, \mu_0) - L \left(\frac{L}{L-l} \right) D_{\mathcal{Q}}(\mu, \mu_k) \leq LD_{\mathcal{Q}}(\mu, \mu_0) \quad (24)$$

Defining:

$$\frac{1}{C_k} = \sum_{k=1}^K \left(\frac{L}{L-l} \right)^k \quad (25)$$

and rearranging the terms leads to:

$$\mathcal{H}(\mu_k) - \mathcal{H}(\mu) \leq C_k LD_{\mathcal{Q}}(\mu, \mu_0) = \frac{\mu D_{\mathcal{Q}}(\mu, \mu_0)}{\left(1 + \frac{l}{L-l}\right)^l - 1} \quad (26)$$

Given Eq. 26, the convergence in the statement can be derived using Lemma 5.1, and the fact that $\left(1 + \frac{l}{L-l}\right)^k \geq 1 + \frac{k\mu}{L-\mu}$. Ultimately, $p_T^\pi \in \mathbb{P}(\Omega_{pre}) \forall \alpha > 0$ is trivially due to the fact that Ω_{pre} is the support of the right element of the Kullback–Leibler divergence in Eq. 9. \square

E PROOF FOR SECTION 7

E.1 PROOF OF THEOREM 7.1

We restate the theorem for reader’s convenience:

Theorem 7.1 (Convergence under general assumptions). *Consider the standard Robbins-Monro step-size rule: $\sum_k \gamma_k = \infty, \sum_k \gamma_k^2 < \infty$. Then under Assumptions 7.3, the sequence of marginal densities p_T^k induced by the iterates π_k of Algorithm 1 converges weakly to p_T^* almost surely. Formally, we have that:*

$$p_T^k \rightharpoonup p_T^* \quad a.s. \quad (18)$$

where $p_T^* \in \arg \max_{p_T \in \mathbb{P}(\Omega_{pre})} \mathcal{H}(p_T)$ is the maximum entropy density compatible with Ω_{pre} .

Proof. To enhance the readability of our proof, we begin by outlining the key steps.

Proof Outline. The main idea is to analyze the convergence of the iterates $\{p_T^k\}_{k \in \mathbb{N}}$ generated by Algorithm 1 by relating them to a corresponding *continuous-time* dynamical system. Specifically, we define the initial dual variable as

$$h_0 = \delta \mathcal{H}(p_{pre}) = -\log p_{pre},$$

and consider the following system:

$$\begin{cases} \dot{h}_t = \delta \mathcal{H}(p_t) \\ p_t = \delta(-\mathcal{H})^*(h_t) \end{cases} \equiv \begin{cases} \dot{h}_t = -\log p_t \\ p_t = \frac{e^{h_t}}{\int_{\Omega} e^{h_t}}. \end{cases} \quad (\text{MF})$$

Here, $(-\mathcal{H})^*(h) := \log \int_{\Omega} e^h$ is the Fenchel dual of the entropy function Hsieh et al. (2019); Hiriart-Urruty & Lemaréchal (2004).

To bridge the gap between discrete and continuous-time analysis, we construct a continuous-time interpolation of the discrete iterates $\{h^k\}_{k \in \mathbb{N}}$. Let $(h^k := \delta \mathcal{H}(p_T^k))_{k \in \mathbb{N}}$ be the sequence of the corresponding *dual variables*. We introduce the notion of an “effective time” τ^k , defined as:

$$\tau^k := \sum_{n=1}^k \gamma_n,$$

which represents the cumulative time elapsed up to the k -th iteration of the discrete-time process h^k using step-size γ_k . Using τ^k , we define the *continuous-time interpolation* $h(t)$ of h^k as follows:

$$h(t) := h^k + \frac{t - \tau^k}{\tau^{k+1} - \tau^k} (h^{k+1} - h^k). \quad (\text{Int})$$

Intuitively, the convergence of our algorithm follows if the following two conditions hold:

Informal Assumption 1 (Closeness of discrete and continuous times). *The interpolated process (Int) asymptotically approaches the continuous-time dynamics in (MF) as $k \rightarrow \infty$.*

Informal Assumption 2 (Convergence of continuous-time dynamics). *The trajectory of (MF) converges to the **optimal solution** of the maximum entropy problem (7).*

To formalize the above intuition, we leverage the *stochastic approximation* framework of Benaïm (2006); Mertikopoulos et al. (2024); Karimi et al. (2024), outlined as follows.

First, to precisely state 1, we introduce a measure of “closeness” between continuous orbits. Let \mathcal{Z} denote the space of integrable functions on Ω (viewed as the dual space of probability measures; see Halmos (2013)), and define the *flow* $\Theta: \mathbb{R}_+ \times \mathcal{Z} \rightarrow \mathcal{Z}$ associated with (MF). That is, for an initial condition $h_0 = h \in \mathcal{Z}$, the function Θ describes the orbit of (MF) at time $t \in \mathbb{R}_+$.

We then define the notion of “asymptotic closeness” as follows:

Definition 2. *We say that $h(t)$ is an asymptotic pseudotrajectory (APT) of (MF) if, for all $T > 0$, we have:*

$$\lim_{t \rightarrow \infty} \sup_{0 \leq s \leq T} \|h(t+s) - \Theta_s(h(t))\|_{\infty} = 0. \quad (27)$$

This comparison criterion, introduced by Benaïm & Hirsch (1996), plays a central role in our analysis. Intuitively, it states that $h(t)$ eventually tracks the flow of (MF) with arbitrary accuracy over arbitrarily long time windows. Consequently, if (Int) is an APT of (MF), we can reasonably expect its behavior—and thus that of $\{h^k\}_{k \in \mathbb{N}}$ —to closely follow (MF).

The precise connection is established by Benaïm & Hirsch (1996) through the concept of *internally chain-transitive* (ICT) sets:

Definition 3 (Benaïm & Hirsch, 1996; Benaïm, 2006). *Let \mathcal{S} be a nonempty compact subset of \mathcal{Z} . Then:*

1. \mathcal{S} is invariant if $\Theta_t(\mathcal{S}) = \mathcal{S}$ for all $t \in \mathbb{R}$.
2. \mathcal{S} is attracting if it is invariant and there exists a compact neighborhood \mathcal{K} of \mathcal{S} such that $\lim_{t \rightarrow \infty} \text{dist}(\Theta_t(h), \mathcal{S}) = 0$ uniformly for all $h \in \mathcal{K}$.
3. \mathcal{S} is an **internally chain-transitive (ICT)** set if it is invariant and $\Theta|_{\mathcal{S}}$ admits no proper attractors within \mathcal{S} .

The significance of ICT sets lies in (Benaïm, 2006, Theorem 5.7):

Theorem E.1 (APTs converge to ICT sets). *Let $h(t)$ be a precompact asymptotic pseudotrajectory generated by $\{h^k\}_{k \in \mathbb{N}}$ for the flow associated with the continuous-time system (MF). Then, almost surely, $h^k \rightarrow \mathcal{S}$, where \mathcal{S} is an ICT set of (MF).*

By Theorem E.1, establishing Theorem 7.1 reduces to proving the following two statements:

1. The iterates $\{h^k\}_{k \in \mathbb{N}}$ of Algorithm 1 generate a precompact APT of (MF).
2. The unique ICT set of (MF) is the solution to the optimization problem (7).

These results provide the rigorous counterpart to 1 and 2. The proof below proceeds by formally establishing each of these points.

The ICT set of (MF) is the solution to (7). By the definition (MF), we can easily see that:

$$\dot{p}_t = p_t \dot{h}_t - \frac{e^{h_t}}{\int_{\Omega} e^{h_t}} \cdot \frac{\int_{\Omega} \dot{h}_t \cdot e^{h_t}}{\int_{\Omega} e^{h_t}} \quad (28)$$

$$= p_t \left(\dot{h}_t - \mathbb{E}_{p_t} \dot{h}_t \right). \quad (29)$$

We then compute:

$$-\frac{d}{dt} \mathcal{H}(p_t) = -\langle \delta \mathcal{H}(p_t), \dot{p}_t \rangle \quad (30)$$

$$= \langle \log p_t, p_t \left(\dot{h}_t - \mathbb{E}_{p_t} \dot{h}_t \right) \rangle \quad \text{by (29)} \quad (31)$$

$$= \int_{\Omega} p_t \log p_t \dot{h}_t - \int_{\Omega} p_t \log p_t \cdot \int_{\Omega} p_t \dot{h}_t \quad (32)$$

$$= - \int_{\Omega} p_t (\log p_t)^2 - \left(\int_{\Omega} p_t \log p_t \right)^2 \quad \text{by (MF)} \quad (33)$$

$$= - \left(\mathbb{E}_{X_t \sim p_t} (\log p_t(X_t))^2 - (\mathbb{E}_{X_t \sim p_t} \log p_t(X_t))^2 \right) \quad (34)$$

$$\leq 0 \quad (35)$$

by Jensen's inequality. Also, note that the inequality is strict if h_t is not constant, i.e., if p_t is not uniform on Ω .

In short, we established in (35) that $\mathcal{H}(\cdot)$ serves as a *Lyapunov function* for the continuous-time system (MF). Since $\mathcal{H}(\cdot)$ is *strictly concave*, the only ICT set is the singleton $\{p_T^*\}$, where p_T^* represents the uniform (and hence entropy-maximizing) measure on Ω (Benaïm, 2006, Proposition. 6.4).

Algorithm 1 generates an APT. Let $(p_T^k)_{k \in \mathbb{N}}$ be the sequence of measures on Ω generated by Algorithm 1 with the oracle `LINEARFINETUNINGSOLVER`, and recall that its dual variables are given by $(h^k := \delta\mathcal{H}(p_T^k))_{k \in \mathbb{N}}$. Also, recall the corresponding continuous-time interpolation (Int).

Assumption 7.1 ensures that each dual variable h^k is a well-defined function on Ω , while Assumption 7.2 guarantees the precompactness of $h(\cdot)$. Furthermore, under Assumption 7.3, standard arguments (see, e.g., **Proposition 4.1** of Benaïm (2006) or Karimi et al. (2024)) establish that $h(\cdot)$ generates an APT of the continuous-time flow defined by (MF). Finally, Theorem E.1 ensures that $\{h^k\}_{k \in \mathbb{N}}$ converges almost surely to an ICT set of (MF), which we have already shown to contain only $\{p_T^*\}$.

Therefore, applying the theory of Hsieh et al. (2021); Karimi et al. (2024), we conclude that, almost surely,

$$\lim_{k \rightarrow \infty} h^k = \lim_{k \rightarrow \infty} \delta\mathcal{H}(p_T^k) = \lim_{k \rightarrow \infty} -\log p_T^k = \delta\mathcal{H}(p_T^*) \quad \text{in } L_\infty. \quad (36)$$

Since Ω is compact, (36) implies that, for any smooth test function ψ on Ω , $\langle p_T^k, \psi \rangle \rightarrow \langle p_T^*, \psi \rangle$, which completes the proof. \square

F DETAILED EXAMPLE OF ALGORITHM IMPLEMENTATION

F.1 PSEUDOCODE FOR IMPLEMENTATION OF EQ. (9)

For the sake of completeness, in the following we present the pseudocode for a possible implementation of a LINEARFINETUNINGSOLVER via a first-order optimization method, used to solve (9), as well as within S-MEME. In particular, we present the same implementation we use in Sec. 8, based on Adjoint Matching (Domingo-Enrich et al., 2024), which captures the linear fine-tuning via a stochastic optimal control problem and solves it via regression.

In the following, we adopt the notation from the Adjoint Matching paper (Domingo-Enrich et al., 2024, Apx E.4). We denote the pre-trained noise predictor by ϵ^{pre} , the fine-tuned one as $\epsilon^{\text{finetuned}}$, and with $\bar{\alpha}$ the cumulative noise schedule, as used by Ho et al. (2020). The complete algorithm is presented in Algorithm 2. First, notice that given a noise predictor ϵ (as Defined in Sec. 2) and a cumulative noise schedule $\bar{\alpha}$, one can define the score s as follows (Song & Ermon, 2019):

$$s(x, t) := -\frac{\epsilon(x, t)}{\sqrt{1 - \bar{\alpha}_t}} \quad (37)$$

Algorithm 2 LINEARFINETUNINGSOLVER (Implementation based on Adjoint Matching (Domingo-Enrich et al., 2024))

- 1: **input:** N : number of iterations, ϵ^{pre} : pre-trained noise predictor, α regularization coefficient, m : trajectories batch size, ∇f : reward function gradient
- 2: **init:** $\epsilon^{\text{finetuned}} := \epsilon^{pre}$ with parameter θ
- 3: **for** $n = 0, 2, \dots, N - 1$ **do**
- 4: Sample m trajectories $\{X_t\}_{t=1}^T$ according to DDPM (Song et al., 2020), e.g., sample $\epsilon_t \sim \mathcal{N}(0, I)$, $X_0 \sim \mathcal{N}(0, I)$

$$X_{t+1} = \sqrt{\frac{\bar{\alpha}_{t+1}}{\bar{\alpha}_t}} \left(X_t - \frac{1 - \frac{\bar{\alpha}_t}{\bar{\alpha}_{t+1}}}{\sqrt{1 - \bar{\alpha}_t}} \epsilon^{\text{finetuned}}(X_t, k) \right) + \sqrt{\frac{1 - \bar{\alpha}_{t+1}}{1 - \bar{\alpha}_t}} \left(1 - \frac{\bar{\alpha}_t}{\bar{\alpha}_{t+1}} \right) \epsilon_t$$

Use reward gradient:

$$\tilde{a}_T = \nabla f(X_T)$$

For each trajectory, solve the lean adjoint ODE, see (Domingo-Enrich et al., 2024, Eq. 38-39), from $t = T$ to 0:

$$\tilde{a}_k = \bar{a}_{t+1} + \bar{a}_{t+1}^\top \nabla_{X_t} \left(\sqrt{\frac{\bar{\alpha}_{t+1}}{\bar{\alpha}_k}} \left(X_t - \frac{1 - \frac{\bar{\alpha}_t}{\bar{\alpha}_{t+1}}}{\sqrt{1 - \bar{\alpha}_t}} \epsilon^{\text{pre}}(X_t, k) \right) - X_t \right)$$

Where X_t and \tilde{a}_t are computed without gradients, i.e., $X_t = \text{stopgrad}(X_t)$, $\tilde{a}_t = \text{stopgrad}(\tilde{a}_t)$. For each trajectory compute the Adjoint Matching objective (Domingo-Enrich et al., 2024, Eq. 37):

$$\mathcal{L}(\theta) = \sum_{t=0}^{T-1} \left\| \sqrt{\frac{\bar{\alpha}_{t+1}}{\bar{\alpha}_t (1 - \bar{\alpha}_{t+1})}} \left(1 - \frac{\bar{\alpha}_t}{\bar{\alpha}_{t+1}} \right) \left(\epsilon^{\text{finetuned}}(X_t, k) - \epsilon^{\text{pre}}(X_t, k) \right) - \sqrt{\frac{1 - \bar{\alpha}_{t+1}}{1 - \bar{\alpha}_t}} \left(1 - \frac{\bar{\alpha}_t}{\bar{\alpha}_{t+1}} \right) \bar{a}_t \right\|^2$$

Compute the gradient $\nabla_\theta \mathcal{L}(\theta)$ and update θ .

- 5: **end for**
 - 6: **output** fine-tuned noise predictor $\epsilon^{\text{finetuned}}$
-

G EXPERIMENT DETAILS

In this section we provide further details on the experiments.

Illustrative setting. For this experiment we ran S-MEME for 6000 gradient steps in total, for $K = 1, 2, 3, 4$. Notably, $k=1$ amounts to having a fixed reward for fine-tuning, $-\log p_T^{pre}(x)$. Each round of S-MEME performs $6000/K$ for the particular experiment. In this way we observe the effect of having more rounds of the mirror descent scheme, with same number of gradient updates. Wince we utilize Adjoint Matching (Domingo-Enrich et al., 2024) for the linear solver in Algorithm 1, we perform an iteration of Algorithm 2 by first sampling 20 trajectories via DDPM of length 400 that are used for solving the lean adjoint ODE with the reward $-\lambda \nabla \log p_T(x)$ and $\lambda = 0.1$. Subsequently we perform 2 stochastic gradient steps by the Adam optimizer with batch size 2048, initialized with learning rate 4×10^{-4} . For the density plots in Figure 2 we sampled 80000 points with 100 DDPM steps. To obtain Figure 2d, we computed a Monte-Carlo estimate of $\mathcal{H}(p_T^{\pi_k})$ with an approximation of $\log p_T^{\pi_k}(x)$ resulting from the instantaneous change of variables and divergence flow equation,

$$\log p(x) = \log p_0(x) + \int_0^T \nabla \cdot f(x_t, t) dt, \quad (38)$$

where f is the velocity of the probability-flow ODE for the variance-preserving forward process of the diffusion.

Text-to-image architecture design. For obtaining Figure 3, similarly as in the illustrative example we used Algorithm 2 as the linear solver. At each iteration of Algorithm 2 we sample 4 trajectories of length 60 by DDPM, conditioned on the prompt on top of which we perform 10 Adam steps with initial learning rate 3×10^{-7} and batch size 8. Each iteration of Algorithm 1 entails 20 iterations of Algorithm 2. We ran Algorithm 1 for $K = 3$. For this experiment, we used $\lambda = 0.1$.

Text-to-image evaluation. Evaluating the entropy of $p_T^{\pi_k}$ is computationally prohibitive for the case of the high-dimensional latent of SD-1.5. Consequently, we opted for proxy metrics to quantify how much does the distribution change with increase of π_k , the FID score for distributional distance and CLIP score for semantic alignment. In addition, we computed the cross-entropy in Table 1 between the Gaussians in the Inception-v3 feature space, where the Gaussians were fitted the same way as in computing the FID score. The FID score, cross-entropy and CLIP score have been computed on 3000 samples from respective conditional distributions.

H ADDITIONAL TEXT-TO-IMAGE RESULTS

In the following, we present additional experimental results obtained via the same text-to-image pre-trained diffusion model introduced in Sec. 8, and with experimental details as presented within Sec. G.

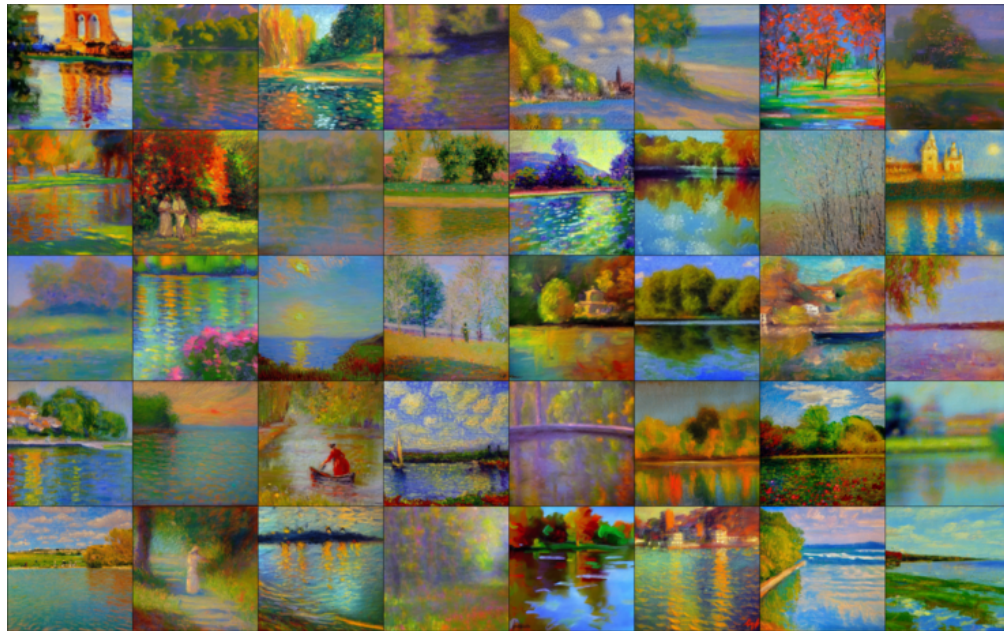


Figure 4: Generated images from π^{pre} with prompt "A creative impressionist painting."



Figure 5: Generated images obtained via fine-tuning of π^{pre} via S-MEME with prompt "A creative impressionist painting."

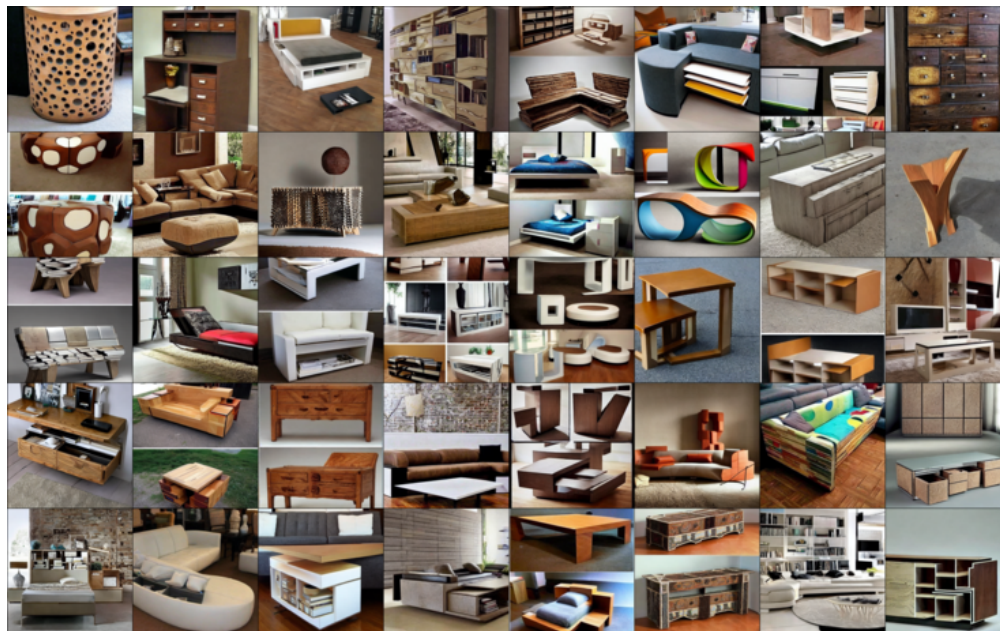


Figure 6: Generated images from π^{pre} with prompt "Creative furniture."

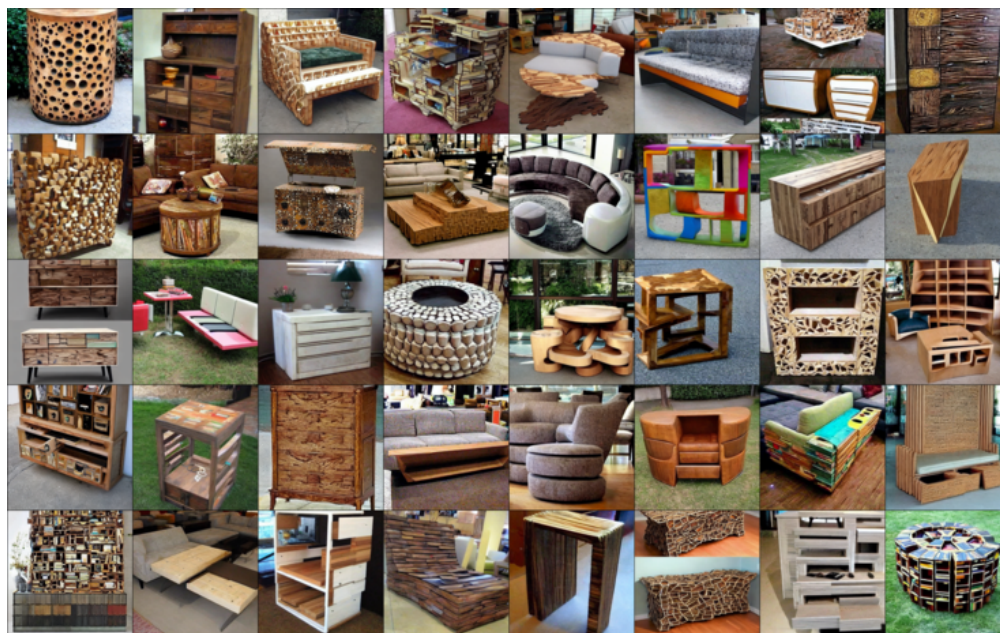


Figure 7: Generated images obtained via fine-tuning of π^{pre} via S-MEME with prompt "Creative furniture."

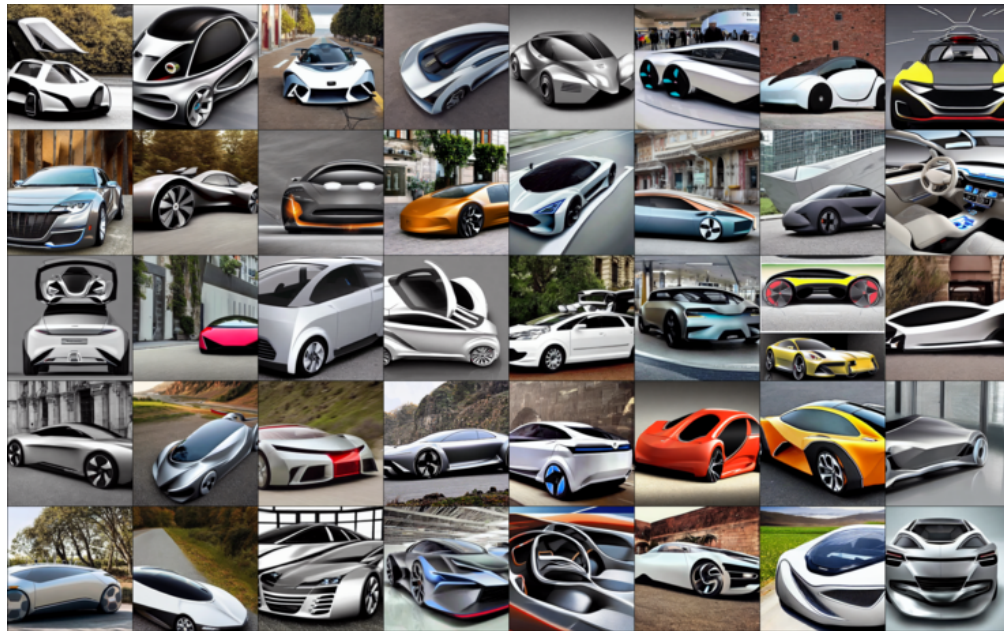


Figure 8: Generated images from π^{pre} with prompt "An innovative car design."

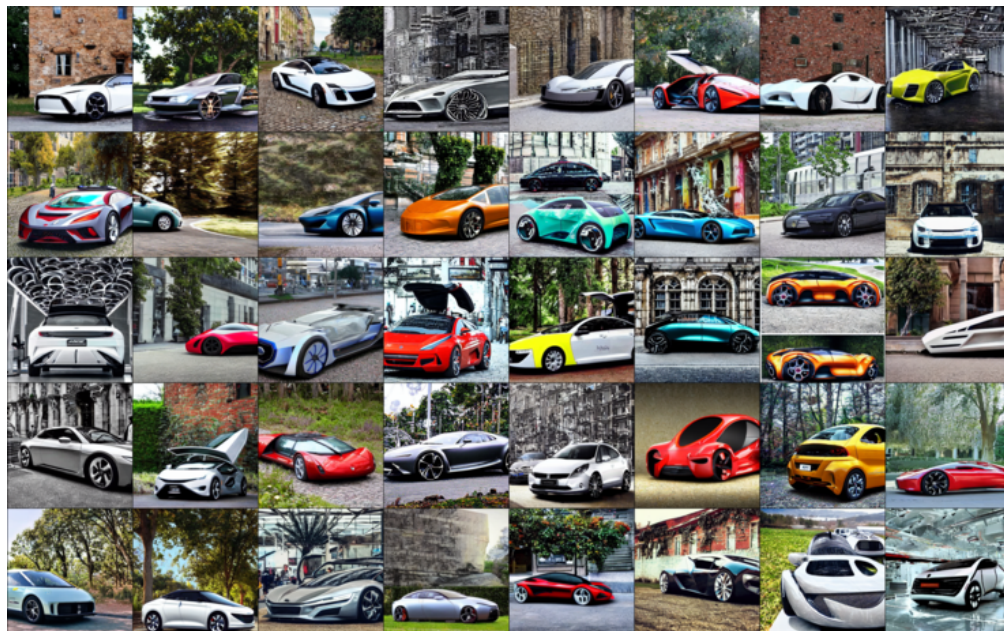


Figure 9: Generated images obtained via fine-tuning of π^{pre} via S-MEME with prompt "An innovative car design."